Eur Biophys J (1986) 13: 373–381

European Biophysics Journal

The homonuclear Overhauser effect in H_2O solution of low-spin hemeproteins

Assignment of protons in the heme cavity of sperm whale myoglobin

J. T. J. Lecomte and G. N. La Mar*

Department of Chemistry, University of California, Davis, California 95616, USA

Received September 16, 1985/ Accepted in revised form December 16, 1985

Abstract. Proton-proton Overhauser effects were observed in ^1H_2O solutions of sperm whale metcyano myoglobin. Dipolar connectivities involving hyperfine-shifted exchangeable protons such as the proximal and distal histidine ring NH's allowed us to categorize signals as arising from residues located on one side of the heme plane or on the other. With these connectivities, as well as spin-lattice relaxation times, spectral assignments were reached that were used to derive structural and dynamic information about the heme environment. Thus, it was shown that the distal histidine residue does not titrate down to pH $\sim$ 4.1 and that the $^{\beta}CH_2$ of the proximal histidine side chain tumbles with the same correlation time as the protein. Some other applications and limitations are presented.

Key words: Myoglobin, nuclear Overhauser effect, exchangeable protons, histidines

Introduction

Paramagnetic derivatives of hemoproteins such as sperm whale Mb[1] in its metcyano form present particularly interesting proton NMR spectra because the short-range electron-nucleus interactions, which cause hyperfine shifts primarily for the nuclei in the heme cavity, facilitate the resolution of active site signals from the intense diamagnetic enevelope. However, the resolution improvement is accompanied by accelerated relaxation times and this second characteristic entails severe difficulties in assigning the resonances. Since peak identification is indispensable to define the heme/protein interactions from both a structural and a dynamic perspective, a number of ad hoc solutions have been applied to the spectral assignment problem.

The use of isotope labeled hemes, for example, has provided a direct way to identify the porphyrin side chain signals (Mayer et al. 1974; Krishnamoorthi 1983). While efficient and unambiguous, this method cannot yield any information on the protein matrix. The initial approach to this other aspect of the problem made use of the hyperfine shifts of paramagnetically relaxed exchangeable protons (Sheard et al. 1970). Four such signals, necessarily arising from protons located in the heme cavity, are readily resolved in mammalian metcyano myoglobins. The analysis of both their shift and relaxation behavior has resulted in the assignment of two of them to the proximal histidine (F8), and one each to the ring NH's of the distal histidine (E7) and possibly histidine FG3, stacked over pyrrole III on the proximal side of the heme (Fig. 1). Differential paramagnetic relaxation is effective in assigning the ring NH's of the F8 and E7 histidines because the paramagnetic influence is dominant (Cutnell et al. 1981) and hence the relative spin-lattice relaxation time depends upon the relative values of R, the proton-iron distance, through

$$T_{1i}/T_{1j} = R_i^6/R_j^6 . \quad (1)$$

The two other hyperfine NH peaks could only be shown to be consistent with proposed assignments (Sheard et al. 1970; Cutnell et al. 1981).

The interproton Overhauser effect (NOE) has led to the identification of a few protein resonances (Johnson et al. 1983; Ramaprasad et al. 1984). As for the T_1 analysis, heme side chains provide the reference signals and the identified peaks arise from nuclei lying in the heme periphery. So far, conspicuous by their absence among assigned non-exchangeable signals are protons of the proximal

* To whom offprint requests should be sent

1 Abbreviations used: *DSS*, 2,2-dimethyl-2-silapentane-5-sulfonate; *Mb*, myoglobin; *NMR*, nuclear magnetic resonance; *NOE*, nuclear Overhauser effect; *ppm*, part per million

and distal histidines, two residues which are thought to play crucial roles in modulating the reactivity of the iron. A conceivably powerful method for assigning these non-labile proton resonances is the detection of NOE's obtained by saturation of the known labile protons from the corresponding residues or, reciprocally, the detection of NOE's to the known labile protons caused by saturation of other spins. Recent work on high-spin ferric myoglobin has shown that NOE's are observable even among strongly paramagnetically relaxed pairs of protons (Unger et al. 1985a). Although labile proton signals in myoglobin generally exhibit exchange rates with bulk water contributing to their relaxation behavior over a wide portion of the pH range, such rates may be sufficiently slow to allow for selective saturation and magnetization transfer via NOE's.

The nuclear Overhauser effect is a process occurring through space by a dipolar mechanism. In a system of two cross-relaxing spins i and j, the internuclear distance r_{ij} can be calculated from the magnitude of the NOE from i to j, $\eta_{i\to j}$, according to the following equations (Noggle and Shirmer 1971):

$$\eta_{i\to j} = \sigma_{ij}\, T_{1j}^{s}\,, \tag{2}$$

where T_{1j}^{s} is the selective T_1 of spin j, and σ_{ij}, the cross-relaxation rate of the pair (ij) in the slow motion limit is given by

$$\sigma_{ij} = -\,(\gamma_H^4\,\hbar^2\,\tau_c)/(10\,r_{ij}^6)\,, \tag{3}$$

where τ_c is the correlation time of the ij vector. The cross-relaxation rate can also be extracted from the initial slope of the NOE build-up in the truncated NOE experiment (Dobson et al. 1982). The equation used is

$$\mathrm{d}\eta_{i\to j}(t)/\mathrm{d}t\,|_{t=0} = \sigma_{ij}\,. \tag{4}$$

We present herein the results of a study based on nuclear Overhauser effects involving the four hyperfine shifted labile proton signals shown in the 24 ppm to 12 ppm window of A in Fig. 2. We provide a confirmation of earlier assignments for three signals and suggest a revision for the tentative fourth one. The identification of the two axial histidine signals permits us to assess the internal mobility of the proximal histidine and the titration behavior of the distal histidine. We also investigate the scope and limitations of the method.

Materials and methods

Myoglobin from sperm whale skeletal muscle was purchased from Sigma Chemical Co. and used without further purification. NMR experiments were performed on concentrated samples (6 mM) in 90% H_2O/10% ^2H_2O 0.2 M in NaCl; the metcyano form was prepared by addition of excess of KCN. The pH was adjusted to the desired value by addition of 0.1 M NaOH or HCl in 90% H_2O/10% ^2H_2O, the pH of the sample was read with a Beckman Model 3550 pH meter equipped with an Ingold microcombination electrode. The values reported for ^2H_2O solutions are not corrected for isotope effect.

Proton NMR spectra were recorded in the FT quadrature mode on a Nicolet NT-500 spectrometer. The bandwidth was set to 15 kHz, 8 K or 16 K data points were collected with 16-bit digitization. The NOE experiments were performed according to

$$(A\,[t_1 - t_{on} - P - A\,c\,q]_n\,B\,[t_1 - t_{off} - P - A\,c\,q]_n)_m\,,$$

where A and B designate two different data files, t_1 is a preparation time to allow the relaxation of the resonances of interest (1 to 1.5 s), t_{on} is the time during which the resonance is kept saturated (typically, saturation is reached within the first 20 ms and t_{on} is set to 300 ms, the power applied is about 0.2 W), t_{off} is an equal time during which the decoupler is set off-resonance. P, the observe pulse was either a Redfield 2-1-4-1-2 excitation (Redfield et al. 1975) or a 1-3-3-1 pulse train (Hore 1983). In both cases some attenuation of the transmitter power was applied to obtain a $\pi/2$ pulse at the carrier (2-1-4-1-2) or to obtain a reliable 1-pulse ($< 11°$, 1-3-3-1); n was set to 64 and the total number of scans in each file ($n * m$) was at least 1,024. The NOE difference spectrum was obtained by subtracting B from A. Truncated NOE experiments were performed with a t_{on} (and t_{off}) ranging from 20 ms to 300 ms. Non-selective T_1 values were measured by the inversion-recovery method (Vold et al. 1968) whereas selective T_1 values were determined by the inversion- or saturation-recovery method. Recovery data were analyzed with a three-parameter non-linear least-squares fit. Chemical shifts are reported in parts per million with reference to DSS.

Results and discussion

Figure 1 shows a schematic representation of the histidine residues closest to the porphyrin ring (distal E7, proximal F8, and FG3). A small stretch of the F helix peptide backbone is included as well. Other pocket residues are not depicted but it should be apparent that because of steric interactions with the heme and the E7 and F8 histidines, the side chains located below the heme are several Å away from those above. Since a primary NOE is not expected between protons lying more than 6 Å apart,

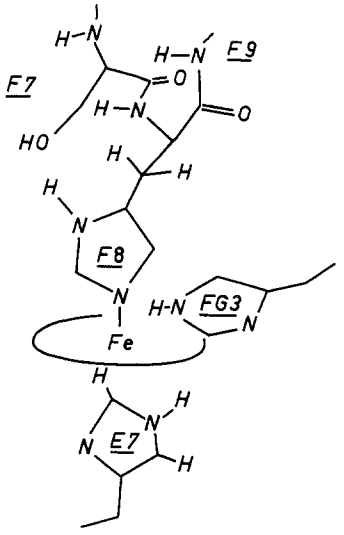

Fig. 1. Schematic representation of the heme environment in sperm whale metcyano myoglobin. Three histidine residues are included: distal (E7), proximal (F8), and FG3. A short stretch of F helix with the two side chains nearest to the proximal histidine, *Ser* F7 and *Ala* F9, is also shown (after Hanson and Schoenborn 1981)

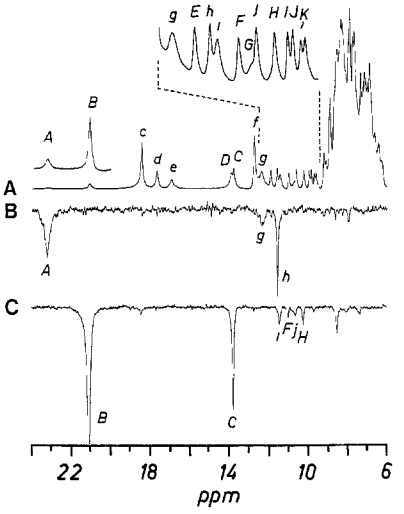

Fig. 2. **A** Portion of the downfield hyperfine-shifted region of the 500 MHz proton spectrum of sperm whale metcyano myoglobin recorded in 90% ^1H_2O/10% ^2H_2O with a Redfield excitation (Redfield et al. 1975) at 30 °C, pH 9.2. Exchangeable protons are labeled with capital letters. Known assignments are as follows: *A*, distal *His* E7 N_3H; *B*, proximal *His* F8 N_1H; *c*, 1-CH_3; *d*, 2-α-vinyl; *D*, *His* FG3 N_3H (tentative); *C*, *His* F8 peptide N*H* (tentative); *f*, 8-CH_3. **B** NOE difference spectrum obtained when irradiating the distal *His* E7 N_3H (*A*) for 300 ms (×100). **C** NOE difference spectrum obtained when irradiating the proximal *His* ring N_1H for 300 ms (×50)

the dipolar connectivities observed from or to the E7 and F8 histidines should define two non-interacting networks of protons. Therefore, the NOE's should allow us to sort several hyperfine-shifted signals as belonging to either the distal or the proximal side. Furthermore, the observation of dipolar contacts with heme side chains, combined with complementary data collected in ^2H_2O can be used to localize more precisely the nuclei under investigation and reinforce the spectral assignments.

Figure 2A presents a portion of the downfield hyperfine-shifted spectrum of MbCN recorded in H_2O with a Redfield excitation. Non-exchangeable heme signals appear in the following order of decreasing chemical shift: 5-CH_3 (at 27 ppm, not shown), 8-CH_3, 2-α vinyl, and 1-CH_3; they are labeled on the spectrum. Capital letters refer to exchangeable protein protons. Signals *A* and *B* have been assigned to the ring N*H* of the distal (E7) and the proximal (F8) histidines, respectively, by chemical shift calculations (Sheard et al. 1970) and spin-lattice relaxation measurements (Cutnell et al. 1981). Comparison with Mb homologues confirmed this view as *B* is always recorded with practically unchanged chemical shift – as expected from a proximal histidine ring N_1H peak – and *A*, which has a more variable shift, is not detected in elephant myoglobin (Krishnamoorthi et al. 1984), a variant with a glutamine instead of a histidine at the E7 position. Signal *C* was tentatively assigned to the peptide N*H* of the proximal histidine whereas *D* has been proposed to arise from the ring N*H* of another histidine residue on the basis of its exchange behavior (Sheard et al. 1970). Assignment to the ring N_3H of histidine FG3 has been found consistent with existing data (Cutnell et al. 1981). Exchangeable protons H_A to H_D were irradiated to observe the corresponding NOE's. The results are as follows.

Distal side: histidine E7

Peak *A* in Fig. 2A arises from the ring N_3H of histidine E7, the distal histidine. Figure 2B presents the NOE difference spectrum obtained when irradiating that exchangeable peak. The steady-state effect is remarkably selective: only a small number of peaks appear in the spectrum. The signals having altered intensity must therefore arise from nuclei located in the immediate vicinity of the saturated spin. In particular, the non-exchangeable one-proton peak *h* and three-proton peak *g* should be assigned to distal residues. The change in intensity of *h* is readily observable as it reaches −5% under the chosen conditions of pH, temperature, and partial saturation of *A*. The steady-state NOE from *A* to *h* can be calculated for complete saturation of *A*, the value obtained is −10%. The selective T_1 of *h* has been determined by saturation-recovery and found to be equal to 69 ± 7 ms (30 °C, pH = 9.2). This value can be

used in Eq. (2) to yield a ca. 1.4 Hz cross-relaxation rate between H_A and H_h. Assuming that the r^{-6} dependence of σ applies in this case (Eq. (3)) and that there is no internal motion ($\tau_c \approx 9$ ns (Marshall et al. 1980, with appropriate temperature corrections; Gilman 1979)), the distance separating the two nuclei can be estimated at about 2.6 Å. Both the C_4 and C_2 protons of the imidazole ring of the distal histidine are at 2.56 Å from the N_3H proton and are likely candidates for *h*. The two protons, however, lie at different distances from the iron atom, the C_2H is at 4.1 Å whereas the C_4H is at 5.9 Å (Hanson and Schoenborn 1981);[2] the non-selective spin-lattice relaxation time of *h* (115 ms), compared to that of the 8-CH_3 (peak *f*, 151 ms) in Eq. (1) yields a R_h of 5.9 Å and therefore favors the C_4H assignment. The only other nuclei close to *His* E7 N_3H, thus constituting candidates for *h*, belong to the *Phe* CD1 ring lying under pyrrole III. Relatively large NOE's are predicted among these aromatic protons since the distance between two of them can be as short as 2.6 Å. Irradiation of *h* yields only small changes of intensity (< 5%) for a small number of peaks (not shown). This observation is inconsistent with the *Phe* CD1 assignment and compatible with the *His* E7 C_4H since, according to the solid state structure of the carbonmonoxy complex (Hanson and Schoenborn 1981), this proton is relatively isolated from other spins.

If the assignment of *h* to the distal histidine C_4H is correct, one must justify the absence of an obvious C_2H signal in the NOE difference spectrum of Fig. 2B, as both protons are equidistant from the N_3H. This absence could be rationalized on the basis of larger linewidth and the faster relaxation time expected because of the proximity of the iron atom (4.1 Å, estimated $T_1 = 13$ ms) rendering the NOE smaller [Eq. (2)] and intrinsically more difficult to detect.

Proximal side: histidine F8

Peak *B* in Fig. 2A has been assigned to the ring N_1H of the proximal histidine F8. Irradiation of H_B (Fig. 2C) reveals a larger number of dipolar connectivities. The signal that is most affected is *C*, another exchangeable proton, previously attributed to the peptide N*H* of the corresponding residue (Sheard et al. 1970). The X-ray structure indicates that the orientation of the F8 side chain with respect to the F-helix is such that the peptide N*H* is brought close (2.3 Å) to the ring N_1H and lies at $r > 6$ Å from the iron. The NOE results are consistent with this geometry and the assignment to the peptide N*H* is thereby confirmed.

The transfer of magnetization from the N_1H to the N*H* of histidine F8 is efficient both at pH's where the exchange with bulk water is slow (e.g. pH = 6.3) and at pH's where it is faster (e.g. pH = 10.8). Considering the case where spin H_i is saturated and transfer is observed to the exchangeable H_j, if the experimental conditions are such that the spin-lattice relaxation time and the overall rate of exchange are comparable, the calculation of σ requires a modified Eq. (2): the selective T_1 should be replaced by an effective T_1 which accounts for the magnetization losses due to spin *j* exchange so that

$$\eta_{i\to j} = \sigma_{ij}/(\varrho_j + k)\,. \qquad (5)$$

When *B* is irradiated at pH 6.3 and 30 °C, a −18% NOE is observed to *C*. Under those conditions, the exchange of *C* with the bulk solvent is relatively slow indicating the inefficiency of acid catalysis for the amide proton ($\varrho = 14$ Hz, $k < 1\,s^{-1}$). At pH 10.8, the NOE is within error of the acid value (−16%) and the rate of exchange with water, as determined by a standard saturation transfer experiment (Campbell et al. 1978), is of $17\,s^{-1}$. The σ values obtained at the two different pH's are −2.6 Hz and −4.4 Hz, which lead to $r(H_B - H_C)$ distances of 2.5 and 2.3 Å, values in reasonable agreement. It should be noted that when the exchangeable H_i and H_j are spatially close, as in the case of H_B and H_C, one cannot, a priori, rule out the possibility of direct exchange between the *i* and *j* sites.

In Fig. 2C, other NOE's are observed from *B*, the F8 ring N*H*, that must arise from the proximal histidine residue itself or from nearby residues on the proximal side: the exchangeable H_F, H_G, and H_H, and the non-exchangeable H_i and H_j. Similarly, irradiation of H_C, the peptide N*H* of the proximal histidine, yields NOE's to H_B, as well as to the exchangeable H_F and H_H and the non-exchangeable H_i and H_j. This is shown in Fig. 3B and more clearly in Fig. 3C where the results of off-resonance irradiation of *D* have been subtracted out. Compared to the effects obtained from *B* (Fig. 2C) and judging on the relative intensities $\eta_{B\to i} = -3.6\% < \eta_{C\to i} = -7.5\%$ and $\eta_{B\to j} = -1.3\% \approx \eta_{C\to j} = -1.1\%$, it can be concluded that the H_i is closer to the peptide N*H* than to the ring N_1H, whereas H_j seems located at about the same distance from both. Among the possible non-exchangeable protons near the proximal histidine N_1H and N*H*, we find the geminal pair $^{\beta}CH_2$ of *His* F8. A strong NOE should connect the two partners of the pair since their inter-

2 In our interpretation of the NMR parameters, we rely on the solid state structure of the carbonmonoxy complex (Hanson and Schoenborn 1981) since at this time, the met-cyano structure has not been reported. For our purposes, we do not expect major differences between the two forms of the protein

nuclear separation is only 1.77 Å. Thus if $H_i(H_j)$ belongs to the $^{\beta}CH_2$ pair, then its irradiation should cause a large effect on another single proton signal.

Figure 4 presents the results obtained when saturating H_i at 11.4 ppm in a ^2H_2O solution of metcyanomyoglobin. A steady state NOE of −43% is observed at 6.3 ppm (Fig. 4C). On the other hand, irradiation of H_j at 10.6 ppm, although yielding some NOE's, does not lead to any effect larger than a few percent (not shown). This indicates that *i* is indeed one of the geminal β protons of *His* F8, the proton located closer to the peptide N*H* (*C*). The solid state structure also shows that this proton we now assign to peak *i* is closer to the peptide N*H* (2.6 Å) than it is to the ring N_1H (2.9 Å), in agreement with the magnitude of the NOE's recorded from *C* and *B*, respectively.[3]

Proximal side: histidine FG3?

The peak labeled *D* in Fig. 2A has been assigned tentatively to the ring N*H* of a histidine residue because of its *H* exchange behavior (Sheard et al. 1970). Its chemical shift exhibits only a slight temperature dependence, which indicates a small, if any, paramagnetic contribution. This could be due to either a large *R* (H_D-Fe) value or a magic angle orientation of the H_D-Fe vector. Sheard et al. (1970) favored the first interpretation and proposed assignment to a buried hydrogen-bonded histidine, namely *His* B5. On the basis of chemical shift and linewidth considerations, Cutnell et al. (1981) suggested that the second interpretation is consistent with the assignment to *His* FG3 (Fig. 1). When H_D is irradiated, it gives rise to a small number of NOE's (Fig. 3D, and Fig. 3E where the off-resonance

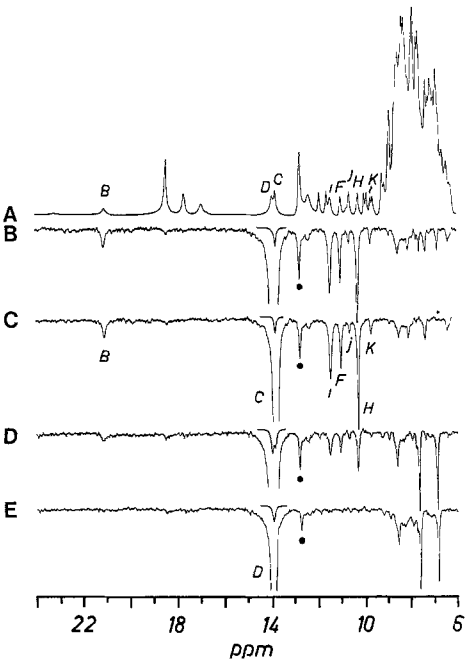

Fig. 3. **A** Reference spectrum identical to that displayed in Fig. 2A. **B** NOE difference spectrum obtained when irradiating *C* (proximal *His* peptide NH) for 300 ms (×50). **C** Same as **B** with computer subtraction of the off-resonance effects introduced by partial saturation of *D*. The peaks discussed in the text are labeled. **D** NOE difference spectrum obtained when irradiating *D* for 300 ms (×50). **E** Same as **D** with computer subtraction of the off-resonance effects introduced by partial saturation of *C*. A *filled circle* denotes off-resonance perturbation (spillage)

effects arising from the simultaneous perturbation of peak *C* have been corrected for). In particular, two signals, at 7.61 ppm and 6.84 ppm, experience an effect of about equal intensity in the difference spectrum. Both lines are sharp and the results of NOE experiments carried out as a function of temperature show that their chemical shifts vary by only 0.04 ppm between 45 °C and 30 °C. The small dependence on temperature and the narrow linewidth indicate minor paramagnetic contributions and suggests that the protons responsible for the signals are relatively remote from the iron center.

Although because of severe overlap, it is somewhat difficult to estimate the intensity of the 7.6 and 6.8 ppm signals in the reference spectrum, they appear as single-proton peaks. The observation of an NOE from a labile proton to two sharp one-proton singlets is characteristic of a histidine ring N_3H (Stoesz et al. 1979; Wu et al. 1984) in dipolar contact with both the C_2H and the C_4H. A natural assignment for these two peaks is then the corresponding C_2H and C_4H. According to the solid state structure, histidine FG3 is located above pyrrole III, parallel to the ring (Fig. 1) and its C_2H and C_4H are

3 The $^2J_{\beta\beta}$ value of a free histidine residue is 15.4 Hz (Wüthrich 1976). In cytochrome *c*, the $^{\beta}CH_2$ pair of *His* 18 exhibits a geminal coupling of 11.7 Hz (Moore and Williams 1984). To confirm our assignment, we attempted a spin-spin decoupling experiment. As peak *z* appears in a crowded region of the spectrum, the decoupling field was applied to *i* during the acquisition of the two spectra required to obtain the NOE from *i* to *z*. This technique allows us to observe *z* in the absence of overlap and to determine its linewidth accurately. No sharpening of the *z* line was observed upon decoupling of *i*. Similarly, application of the decoupling field at 6.3 ppm during a normal collection did not lead to any sharpening of the *i* line. To understand the absence of spin-spin coupling between *i* and *z*, the selective T_1 of peak *i* was measured. The value obtained, 30 ms, correspond to a rate of 33 Hz. The selective T_1 of *z*, extracted from the truncated experiment, corresponds to a 34 Hz rate. These rates are fast compared to $J/(1.41)$ (Frankel 1969) and are able to induce decoupling or at least a reduction of the apparent *J* value; the extent of sharpening upon decoupling could be beyond the detection limit. We conclude that this observation does not invalidate the assignment

at 7.3 and 4.6 Å from the iron, respectively. The C_4H is therefore expected to be broad, to relax rapidly (expected $T_1 = 23$ ms), and its chemical shift to experience a large paramagnetic contribution. Thus, the NOE data do not support an assignment to *His* FG3 unless there is a large discrepancy between the solid state description and the solution structure. This is unlikely and H_D is proposed to belong to another histidine – the slight temperature dependence of its chemical shift could arise from the presence of a hydrogen bond.

F helix peptide NH's

The NOE's observed from the proximal histidine peaks *B* (Fig. 2C) and *C* (Fig. 3C) to at least three exchangeable proton peaks *F* (10.96 ppm), *H* (10.22 ppm), and *K* (9.68 ppm), suggest assignment to the peptide N*H*'s of neighbor residues in the F helix, *Ala* F9 (*Ala* 94) and *Ser* F7 (*Ser* 92), and to the hydroxyl O*H* of *Ser* F7 (Fig. 1). As proved useful in the non-exchangeable *i* and *j* analysis (Figs. 2 and 3), comparison of NOE values from different nuclei to a same nucleus allows us to establish a distance relationship in the simplified model of independent two-spin systems. H_C experiences equal magnitude NOE's from both H_F and H_H ($\sim -9\%$) and is therefore equidistant from both protons. Furthermore, a relatively large NOE connects H_F to H_K. The assignments consistent with these observations are as follows: H_F, *Ser* F7 N*H* and H_H, *Ala* F9 N*H*, both rigidly held at 2.6 Å from H_C; and H_K, *Ser* F7 O*H*. This however requires a slight readjustment of the *Ser* F7 hydroxyl position to account for a non-zero NOE from H_t to H_K separated by 4.7 Å according the X-ray structure. Such assignment of exchangeable protons is crucial not only for structural purposes but also for hydrogen exchange studies and can be exploited to describe the dynamics of whole sections of polypeptide chain.

Distal side versus proximal side

Thus far, we have discussed signals arising from a few residues, namely E7, F7, F8, F9, and "FG3". In Figs. 2, 3, and 4, several NOE's are detected that were not analyzed, the assignment of these additional signals will be discussed elsewhere. In the scope of this study, it should simply be emphasized that we did not detect any peak experiencing an NOE from both the distal and the proximal ring N*H*'s, and furthermore, that NOE's do connect the signals classified as "distal" or "proximal". These observations are consistent with the definition of two independent networks of protons.

Titration of the distal histidine

With the above assignment of the *His* E7 C_4H (*h*), a non-exchangeable proton, the pH behavior of the distal residue can be monitored over the whole pH range. The pH dependence of the chemical shift of *h* has been reported previously (Krishnamoorthi and La Mar 1984, Fig. 3, peak *g*), the total deviation is 0.1 ppm between the pH limits of 4.0 and 9. The chemical shift deflection expected for a histidine C_4H upon titration of the imidazole group is about 0.4 ppm (Markley 1975). The small change observed in the case of *h* is unlikely to be due to the E7 residue titration and could reflect the ionization of a nearby residue. On the basis of the assignment of *h* and of its pH response, we conclude that the distal histidine in SWMbCN does not titrate between pH 9 and 4. This is interesting since pK_a values attributed to *His* E7 have been reported for several myoglobin complexes: 5.7 (FeMbCO; Hayashi et al. 1976), 5.8 ($FeMbO_2$; Fuchsman and Appleby 1979), 5.6 ($CoMbO_2$; Ikeda-Saito et al. 1977), 5.5 (FeMbF; Asher et al. 1981), and 4.95 (FeMbCO; Doster et al. 1982). However, these indirectly observed pK_a's may not be connected to *His* E7; the possibility has been reviewed recently by Bradbury and Carver (1984) who favor *His* FG3 titration. Another argument for the *His* FG3 involvement is found in the presence of the titration, reflected in the chemical shift of a heme resonance (5-CH_3), even in met-cyano elephant Mb, a protein lacking the histidine at position E7 (Krishnamoorthi and La Mar 1984). The direct observation of a resonance arising from the distal *His* ring reinforces the view that the pK_a is actually lower than 5.5. Precedence for high acidity of the distal histidine has been reported in the case of carbonmonoxyleghemoglobin, where the pK_a reaches 4.1 (Johnson et al. 1978). In the α-chain of carbonmonoxy hemoglobin A, the pK_a may be lower than 4.8 (Dalvit and Ho 1985).

Histidine side chain dynamics

The steady state NOE's have allowed us to identify two vectors with fixed known length: the N_3H-C_4H of *His* E7 and the ${}^{\beta}CH-{}^{\beta}CH'$ of *His* F8. In a truncated NOE experiment, the magnitude of the effect is monitored as a function of saturation time. Equation (4) indicates that the initial slope of the plot of $\eta_{i\to j}$ versus t is the cross-relaxation rate on the ij pair. Thus, the correlation time of the ij vector (τ_c) can be extracted through Eq. (3). Such a study has been carried on the proximal histidine vector H_t-H_z. Figure 4B and C show the NOE obtained after 30 ms and 300 ms of saturation of spin H_t, it can be seen that H_z intensity is detected at the earliest times. Figure 5 presents the plot of $\eta_{t\to z}$

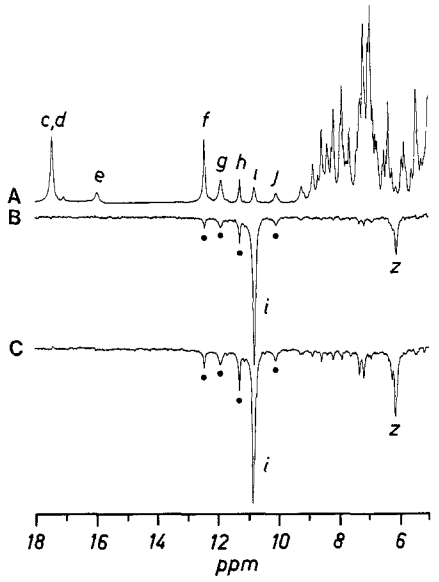

Fig. 4. Truncated NOE experiment carried on metcyano myoglobin in ^2H_2O, 45 °C, pH 7.85. **A** Reference spectrum. **B** NOE difference spectrum obtained after 30 ms complete saturation of peak *i* (×20). **C** NOE difference spectrum obtained after 300 ms complete saturation of *i* (×20). A *filled circle* denotes spillage

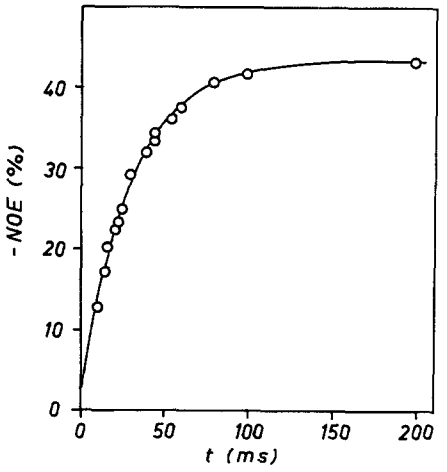

Fig. 5. Proximal histidine β-methylene: plot of the magnitude of the nuclear Overhauser effect versus saturation time in the truncated NOE experiment described in Fig. 4. Analysis of the data yields $\sigma_{iz} = -15$ Hz and $\varrho_z = 34$ Hz

versus saturation time and demonstrates that the effect is primary and σ_{iz} is -15 Hz. With r_{iz} taken equal to 1.77 Å, a correlation time of 8×10^{-9} s is obtained. This correlation time is, within error, equal to the tumbling time of the protein and suggests that the $H_i - H_z$ vector remains fixed with respect to the protein coordinates in the time scale of the NMR experiment.

Similar dynamic studies could be undertaken on the distal residue. The experiment is more difficult as the ring N*H* relaxes faster, and is therefore harder to saturate, and the maximum effect to the C_4H is only -10%. Nevertheless, it should be feasible with the proper instrumentation. A correlation time could then be obtained that would reflect the mobility of this important residue.

Paramagnetic relaxation as a structural probe

Non-selective spin-lattice relaxation rates have been used as structural probes with the assumption that the paramagnetic contribution (ϱ_{para}) dominates the diamagnetic, cross-relaxation, and exchange contributions (ϱ_{dia}, $\Sigma\sigma$, and Σk). Under those conditions, if the scalar contribution to ϱ_{para} is small[4], then ϱ_{para} is proportional to R^{-6} (Eq. (1); Swift 1973). Thus, H_A (*His* E7 ring N_3H), located close to the iron atom, has a large ϱ_{para} and relatively small $\Sigma\sigma$, and at pH 9.2, 30 °C, the k value is smaller than 0.1 ϱ, and its non-selective and selective spin-lattice relaxation times are within experimental error, Eq. (1) can be applied. A 4.2 Å distance is obtained, in very good agreement with the X-ray structure (Cutnell et al. 1981). H_B (*His* F8 ring N_1H) can be identified through similar relaxation considerations as the $\Sigma\sigma$ value is also relatively small. However, cross-relaxation rates as fast as -18 Hz (geminal pair, $\tau_c = 11 \times 10^{-9}$ s) are present in this molecule. Such fast rates are not always negligible in front of ϱ_{para}. Therefore, caution should be applied when using non-selective T_1 for structural determination as cross-relaxation rates might be comparable to ϱ_{para}[5].

Conclusions

Nuclear Overhauser effects have been observed from and among exchangeable protons in low-spin ferric metcyano myoglobin in spite of fast spin lattice relaxation times. These NOE's are particularly interesting as they can be used for various ends: *a)* dipolar connectivities with the proximal and

4 The scalar and delocalized spin density contributions are not always readily estimated (Unger et al. 1985 b)

5 In the evaluation of interproton distances using the value of the cross-relaxation rate σ, we have assumed that the dipolar contribution dominates the zero-quantum transition rate. Recent work on a tightly coupled two-spin system of 6-methylcoumarin has shown that this rate is strongly enhanced by the presence of Gd(III) (Valdez and Jones 1985). Although the nature of the effect is not understood yet, this may suggest that the zero-quantum transition rate is influenced by the paramagnetic center, even in the absence of tight coupling. So far, we have found no indication that this is the case in our work, where we have considered only AX spin systems (weak coupling, $\Delta\delta \gg 10$ J)

distal residues can be established and employed to sort resonances into "distal" and "proximal" categories; *b)* assignments to exchangeable protons can be readily confirmed (*His* F8 N_1H and *His* F8 NH) or found inconsistent with the solid state structure (*His* FG3 N_3H); *c)* the identification of peptide protons offers new probes for kinetics studies; *d)* dynamic studies of the proximal, distal, and other side chains can be undertaken by means of the truncated NOE experiment bearing on constant-length vectors; *e)* titration behaviors can be elucidated by following non-exchangeable protons belonging to ionizable side chains. Furthermore, since for higher molecular weights the spin-lattice relaxation times are essentially the same, the method should also be suitable for a large number of interesting proteins such as tetrameric hemoglobins.

Acknowledgements. This research was supported by grants from National Science Foundation CHE-84-15239 and the National Institutes of Health HL-16087.

References

Asher SA, Adams ML, Schuster TM (1981) Resonance Raman and absorption spectroscopic detection of distal histidine-fluoride interactions in human methemoglobin fluoride and sperm whale metmyoglobin fluoride: Measurements of distal histidine ionization constant. Biochemistry 20: 3339–3346

Bradbury JH, Carver JA (1984) Conformational differences between various myoglobin ligated states as monitored by ^{1}H NMR spectroscopy. Biochemistry 23:4905–4913

Campbell ID, Dobson CM, Ratcliffe RG, Williams RJP (1978) Fourier transform NMR pulse methods for the measurement of slow exchange rates. J Magn Reson 29: 397–417

Cutnell JD, La Mar GN, Kong SB (1981) Proton nuclear magnetic resonance study of the relaxation behavior and kinetic lability of exchangeable protons in the heme pocket of cyanometmyoglobin. J Am Chem Soc 103:3567–3572

Dalvit C, Ho C (1985) Proton nuclear Overhauser effect investigation of the heme pockets in ligated hemoglobin: conformational differences between oxy and carbonmonoxy forms. Biochemistry 24:3398–3407

Dobson CM, Olejniczak ET, Poulsen FM, Ratcliffe RG (1982) Time development of proton nuclear Overhauser effects in proteins. J Magn Reson 48:97–110

Doster W, Beece D, Bowne SF, DiIorio EE, Eisenstein L, Frauenfelder H, Reinisch L, Shyamsunder E, Winterhalter KH, Yue KT (1982) Control and pH dependence of ligand binding to heme proteins. Biochemistry 21:4831–4839

Frankel LS (1969) NMR investigation of relaxation and "chemical exchange spin decoupling" in dilute solutions of Co^{2+} with various "P–O" containing solvents. J Chem Phys 50:943–950

Fuchsman WH, Appleby CA (1979) CO and O_2 complexes of soybean leghemoglobins: pH effects upon infrared and visible spectra. Comparisons with CO and O_2 complexes of myoglobin and hemoglobin. Biochemistry 18:1309–1321

Gilman JG (1979) Carbon-13 nuclear magnetic resonance study of the motional behavior of ethyl isocyanide bound to myoglobin and hemoglobin. Biochemistry 18:2273–2279

Hanson JC, Schoenborn BP (1981) Real space refinement of neutron diffraction data from sperm whale carbonmonoxymyoglobin. J Mol Biol 153:117–146

Hayashi Y, Yamada H, Yamazaki I (1976) Heme-linked proton dissociation of carbon monoxide complexes of myoglobin and peroxidases. Biochim Biophys Acta 427: 608–616

Hore PJ (1983) Solvent suppression in FT NMR. J Magn Reson 55:283–300

Ikeda-Saito MI, Iizuka T, Yamamoto H, Kayne FJ, Yonetani T (1977) Studies on cobalt myoglobins and hemoglobins. Interaction of sperm whale myoglobin and glycera hemoglobin with molecular oxygen. J Biol Chem 252:4881–4887

Johnson RD, Ramaprasad S, La Mar GN (1983) A method of assigning functionally relevant amino acid residue resonances in paramagnetic hemoproteins using proton NOE measurements. J Am Chem Soc 105:7205–7206

Johnson RN, Bradbury JH, Appleby CA (1978) A proton magnetic resonance study of the distal histidine of soybean leghemoglobin. J Biol Chem 253:2148–2154

Krishnamoorthi R (1983) A proton NMR study of the structure and dynamics of some selected heme-proteins. Ph.D. Thesis, University of California, Davis

Krishnamoorthi R, La Mar GN (1984) Identification of the titrating group in the heme cavity of myoglobin. Evidence for the heme-protein $\pi-\pi$ interaction. Eur J Biochem 138:135–140

Krishnamoorthi R, La Mar GN, Mizukami H, Romero A (1984) A ^{1}H NMR comparison of the met-cyano complexes of elephant and sperm whale myoglobin. Assignment of labile proton resonances in the heme cavity and determination of the distal glutamine orientation from relaxation data. J Biol Chem 259:8826–8831

Markley JL (1975) Observation of histidine residues in proteins by means of nuclear magnetic resonance spectroscopy. Acc Chem Res 8:70–80

Marshall AG, Lee KM, Martin PW (1980) Determination of correlation time from perturbed angular correlations of γ rays: Apomyoglobin reconstituted with ^{111}Indium(III)-mesoprotoporphyrin IX. J Am Chem Soc 102:1460–1462

Mayer A, Ogawa S, Shulman RG, Yamane T, Cavaleiro JAS, Rocha-Gonsalves AMd'A, Kenner GW, Smith KM (1974) Assignments of the paramagnetically shifted heme methyl nuclear magnetic resonance peaks of metcyanomyoglobin by selective deuteration. J Mol Biol 86:749–756

Moore GR, Williams G (1984) Assignment of ^{1}H-NMR resonances of the heme and axial histidine ligand of mitochondrial cytochrome *c*. Biochim Biophys Acta 788: 147–150

Noggle JH, Shirmer RE (1971) In: The nuclear Overhauser effect. Academic Press, New York

Ramaprasad S, Johnson RD, La Mar GN (1984) ^{1}H-NMR nuclear Overhauser enhancement and paramagnetic relaxation determination of peak assignment and the orientation of Ile-99 FG5 in metcyanomyoglobin. J Am Chem Soc 106:5330–5335

Redfield AG, Kunz SD, Ralph EK (1975) Dynamic range in Fourier transform proton magnetic resonance. J Magn Reson 19:114–117

Sheard B, Yamane T, Shulman RG (1970) Nuclear magnetic resonance study of cyanoferrimyoglobin; identification of pseudocontact shifts. J Mol Biol 53:35–48

Stoesz JD, Malinowski DP, Redfield AG (1979) Nuclear magnetic resonance study of solvent exchange and nuclear Overhauser effect of the histidine protons of bovine superoxide dismutase. Biochemistry 18:4669–4675

Swift TJ (1973) In: La Mar GN, Horrocks Jr WD, Holm RH (eds) NMR of paramagnetic molecules. Academic Press, New York

Unger SW, Lecomte JTJ, La Mar GN (1985a) The utility of the nuclear Overhauser effect for peak assignment and structure elucidation in paramagnetic proteins. J Magn Reson 64:521–526

Unger SW, Jue T, La Mar GN (1985b) Proton NMR dipolar relaxation by delocalized spin density in low-spin ferric porphyrin complexes. J Magn Reson 61:448–456

Valdez D, Jones CR (1985) Applicability of a random-field model to the $Gd(fod)_3$-induced relaxation of 6-methylcoumarin. J Magn Reson 62:474–486

Vold RL, Waugh JS, Klein MP, Phelps DE (1968) Measurement of spin relaxation in complex systems. J Chem Phys 48:3831–3832

Wu X, Westler WM, Markley JL (1984) The assignment of imidazolium N-^{1}H peaks in the ^{1}H NMR spectrum of a protein by one- and two-dimensional NOE experiments. J Magn Reson 59:524–529

Wüthrich K (1976) In: NMR in biological research: peptides and proteins. North Holland, Amsterdam

Yoshikawa S, O'Keeffe DH, Caughey WS (1985) Investigations of cyanide as an infrared probe of hemeprotein ligand binding sites. J Biol Chem 260:3518–3528

Eur Biophys J (1986) 13: 381

European Biophysics Journal

Erratum

Compact state of a protein molecule with pronounced small-scale mobility: bovine α-lactalbumin

D. A. Dolgikh[1], L. V. Abaturov[2], I. A. Bolotina[2], E. V. Brazhnikov[1], V. E. Bychkova[1], R. I. Gilmanshin[1], Yu. O. Lebedev[2], G. V. Semisotnov[1], E. I. Tiktopulo[1], and O. B. Ptitsyn*[1]

[1] Institute of Protein Research, Academy of Sciences of the USSR, SU-142292 Pushchino, Moscow Region, USSR
[2] Institute of Molecular Biology, Academy of Sciences of the USSR, SU-117312 Moscow, USSR
[3] Institute of Biophysics, Academy of Sciences of the USSR, SU-142292 Pushchino, Moscow Region, USSR

Eur Biophys J (1985) 13: 109–121

Due to an unfortunate printing error, V. N. Bushuev was omitted from the list of authors at the head of the above article.